

# Flat Band and Many-body Gap in Chirally Twisted Triple Bilayer Graphene

Wenlu Lin,<sup>1,\*</sup> Wenxuan Wang,<sup>1,\*</sup> Shimin Cao,<sup>1,\*</sup> Miao Liang,<sup>2</sup> Lili Zhao,<sup>1</sup> Kenji Watanabe,<sup>3</sup> Takashi Taniguchi,<sup>4</sup> Jinhua Gao,<sup>2,5</sup> Jianhao Chen,<sup>1,†</sup> Xiaobo Lu,<sup>1,‡</sup> and Yang Liu<sup>1,5,§</sup>

<sup>1</sup>International Center for Quantum Materials, Peking University, Haidian, Beijing 100871, China

<sup>2</sup>School of Physics and Wuhan National High Magnetic Field Center, Huazhong University of Science and Technology, Wuhan 430074, China

<sup>3</sup>Research Center for Electronic and Optical Materials, National Institute of Material Sciences, 1-1 Namiki, Tsukuba 305-0044, Japan

<sup>4</sup>Research Center for Materials Nanoarchitectonics, National Institute of Material Sciences, 1-1 Namiki, Tsukuba 305-0044, Japan

<sup>5</sup>Hefei National Laboratory, Hefei 230088, China

(Dated: January 14, 2025)

We experimentally investigate the band structures of chirally twisted triple bilayer graphene. The new kind of moiré structure, formed by three pieces of helically stacked Bernal bilayer graphene, has flat bands at charge neutral point based on the continuum approximation. We experimentally confirm the existence of flat bands and directly acquire the gap in-between flat bands as well as between the flat bands and dispersive bands from the capacitance measurements. We discover a finite gap even at zero perpendicular electric field, possibly induced by the Coulomb interaction and ferromagnetism. Our quantitative study not only provides solid evidence for the flat-band and interesting physics, but also introduces a quantitative approach to explore phenomena of similar moiré systems.

The relation between the chemical potential  $\mu$  and the particle density  $n$  is one of the essential properties describing a Fermionic system [1, 2]. Many interesting physics is related to anomalies in this  $\mu$  vs.  $n$  relation, such as the van-Hove singularity and Dirac cone where  $dn/d\mu$  divergies or vanishes [3, 4]. External magnetic field, artificial patterns or electron-phonon interactions can also induce similar anomalies such as heavy Fermions, superconductivity, moiré superlattice, etc. [5, 6]. Many probing methods, e.g. conductivity and commensurability oscillation, etc. [7, 8], can reveal features with proper assumptions such as uniform and constant scattering rate. However, a direct probe of these features is always of fundamental importance for exploring condensed matter systems.

Recently, interests increasingly grow in studying twistrionics materials, where the modulated interlayer coupling leads to abundant features, including flat-band and many-body gaps and so on [9, 10]. The appearance of flat-band is generally believed to be the onset of many interaction induced quantum phases such as fractional quantum Hall effect and Wigner crystal [11]. Signatures of superconductivity-like phenomenon and charge-density waves (so-called “generalized” Wigner crystal) have been reported in these systems [12]. The chirally twisted triple bilayer graphene (CTTBG) has two equal-sized moiré Brillouin zones with a mis-orientation of the rotation angle, generated by the two sets of moiré superlattice [13, 14]. The ultra-flat moiré bands can exist for a relatively wide range of the rotation angle, and are well isolated from other dispersive bands at higher energy, making CTTBG a new platform for exploring interacting physics. When a finite perpendicular electric field

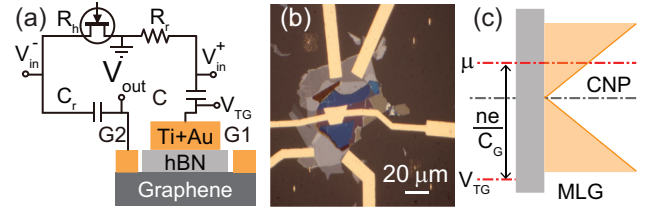


FIG. 1. (a) Schematic diagram of our setup, which measures the capacitance between the top gate (TG) and the contacts. (b) Picture of our monolayer graphene (MLG) sample. (c) Cartoon explaining the measurement principle. The orange shades represent the density of state (DOS) of MLG.

is applied, the intertwined flat valance and conduction bands separate and a band gap at charge neutral point (CNP) develops.

Despite the criticality of the flat-bands in twistrionics devices, firm and direct experimental demonstration of its existence and a direct measure of the moiré superlattice strength are still missing. In this work, we compare the capacitance measured from monolayer graphene (MLG) and CTTBG. We evidence that CTTBG has flat bands coexisting with many-body ferromagnetism gap whose value we can accurately acquire. This intrinsic band gap has been reported in other suspended graphene systems while has not been discovered in such moiré systems [15, 16].

Our CTTBG consists of three pieces of Bernal stacked bilayer graphene chirally stacked on top of each other with the same rotation angle. The two twisted angles are  $1.7^\circ$  so that the supermoiré structure with ultra-large periodicity largely retains the electronic properties dominated by original lattice. The CTTBG is predicted to

host a pair of flat moiré bands well isolated from other dispersive bands at higher energy [12, 17], giving rise to fundamentally different moiré band structures and leading to exotic interaction-induced quantum phenomena.

The measurements are performed in a dilution refrigerator whose base temperature is below 10 mK. The longitudinal resistance  $R_{xx}$  shown in SI is measured using a standard lock-in technique ( $< 30$  Hz) [18]. The capacitance measurements are conducted between top gate (TG) and contacts using a cryogenic bridge, see Fig. 1(a). Capacitance and conductance components can be simultaneously extracted in our capacitance measurements. We have subtracted the parasitic capacitance  $C_p$  (typically about 30 fF) from all present data in this manuscript as long as it's possible and necessary. We measure the parasitic capacitance  $C_p$  by tuning the graphene density to nearly zero and applying a large perpendicular magnetic field (the inset of Fig. 2(b)) when the graphene layer becomes insulating and does not contribute to the capacitance. The Fig. 3(c-d) and 4(c-d) data is taken at constant  $D = 0$  while the Fig. 4(a) data is taken by sweeping  $V_{FG}$  with constant  $V_{BG}$ . In these two cases, the gap  $\Delta$  can be directly read from the width of this minimum  $\Delta V_{TG}$  through  $\Delta = \frac{2K}{1+K} \times \Delta V_{TG}$  or  $\Delta = \frac{K}{1+K} \times \Delta V_{TG}$ , respectively.

We first demonstrate our measurement principle using a MLG device. The TG is separated from the graphene by a thin h-BN layer [19]. The accumulated charge  $ne$  in the two layers ( $e$  is the electron charge and  $n$  is the carrier density) supports an electric potential difference across the insulating layer through the geometric capacitance  $C_G$ , as well as changes the graphene chemical potential by  $\mu$ , see Fig. 1(c). The voltage between the graphene and the gate is the sum of these two components. If the device has an additional bottom gate (BG), the voltage-density relation can be expressed as:

$$(V_{TG} - \mu) \times C_G + (V_{BG} - \mu) \times C_G \times K^{-1} = ne \quad (1)$$

where  $C_G$  is the geometric capacitance (measured between TG and the graphene),  $V_{TG}$  and  $V_{BG}$  are the voltage between the corresponding gates and the graphene.  $K$  is the ratio between the gating efficiencies of the TG and BG, and  $K = \infty$  if the sample has no (or floating) BG.

The AC capacitance  $C$  in Fig 2(a), measured by our bridge using a small excitation [20], is the differential capacitance  $C = e \frac{\partial n}{\partial V_{FG}}$ . Near the Dirac cone, the reduced compressibility  $dn/d\mu$ , i.e. the density of state (DOS) at the Fermi energy, suppresses the graphene's charging capability and leads to a capacitance minima in the zero-field trace of Fig. 2(a) [6, 21–23]. Thus, the dispersion parameter can be derived from the  $dn/d\mu$  quantitatively if the capacitance can be measured with high precision. We note that  $C_G/C = 1 + (dn/d\mu)^{-1} \times \frac{C_G}{e}$ , and  $dn/d\mu = \frac{2e}{\hbar v_F \sqrt{\pi}} \sqrt{n}$  for linear dispersion Dirac Fermions

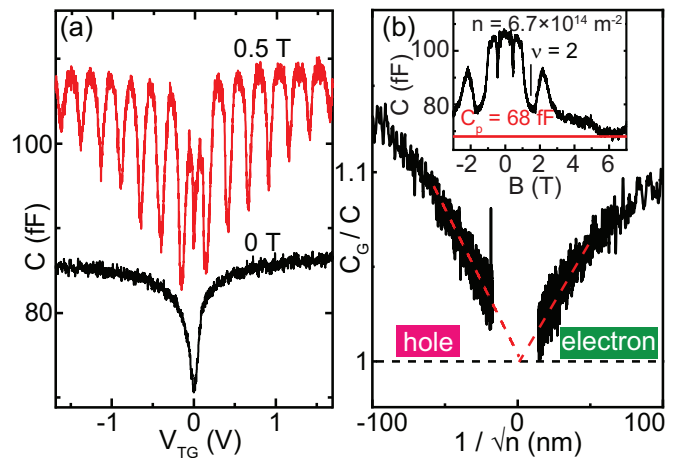


FIG. 2. (a) Capacitance data taken from MLG sample at  $B = 0$  and 0.5 T. (b) The  $C_G/C$  vs.  $1/\sqrt{n}$  plot of the zero magnetic field data in panel (a). The red dashed line is its linear fitting. The inset shows the  $C$  vs.  $B$  at density  $n = 6.7 \times 10^{14} m^{-2}$ . The parasitic capacitance  $C_p \approx 68 fF$  is deduced from the minimum  $C$  value at  $B > 6$  T.

with its Fermi velocity  $v_F$ . Therefore,  $v_F$  can be obtained from our experimental data in the following fashion. We first plot the ratio  $C_G/C$  as a function of  $1/\sqrt{|n|}$ , the positive (negative) value of the  $1/\sqrt{|n|}$  corresponds to electron (hole). The results exhibit linear dependence, directly evidencing the linear dispersion of the Dirac Fermions. The fitting parameter  $C_G$  is the device geometric capacitance. It equals the  $C$  measured at infinitely large  $n$  (and hence infinitely large  $dn/d\mu$ ). Correct  $C_G$  value sets the y-axis intercept of the Fig. 2(b) data to unity. Finally, we can calculate the Fermi velocity  $v_F$  from the slope of the linear fitting, see the red dashed lines in Fig. 2(b).  $v_F$  equals  $1.23 \times 10^6 m/s$  for holes and  $1.14 \times 10^6 m/s$  for electrons. It is worth emphasizing that, the density  $n$  is not proportional to the applied gate voltage because of the varying  $dn/d\mu$ . Instead, the density used in Fig. 2(b) is measured experimentally from quantum oscillations, which we will discuss later.

As pointed out in an earlier work, local compressibility measurement is usually more sensitive than transport measurement [24]. The capacitance data exhibits minimum as soon as a small area of incompressible plaques form inside the samples, while the usual transport measurement can only see features when these plaques form a connected path. We are able to observe clear quantum oscillations at very small magnetic field  $\sim 0.1$  T. When an interger number of Landau levels are occupied, the system's compressibility reduces and a minima appears in the measured  $C$  [25]. We then use the filling factor  $\nu$  and magnetic fields  $B$  of these minima to calculate the exact particle density through  $n = \frac{eB\nu}{h}$  without any fitting parameters. As shown in Eq. 1, the ratio  $V_{TG}/n$  approaches  $eC_G$  as  $|n|$  increases since  $\mu/n$  vanishes. We summarize

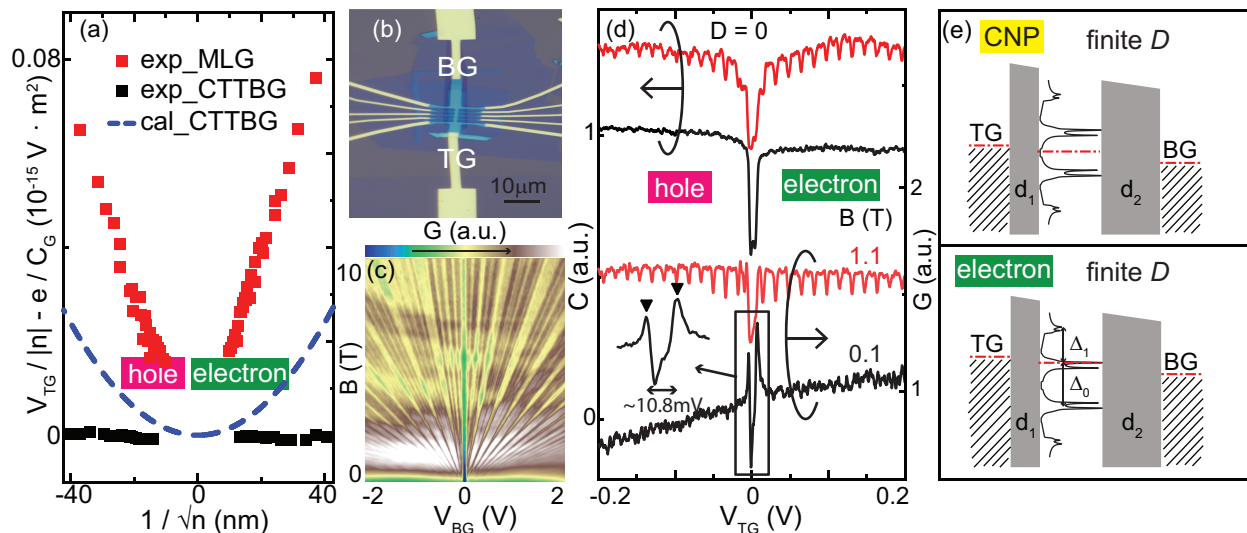


FIG. 3. (a) The  $V_{TG}/n$  vs.  $1/\sqrt{n}$  plot of the data from the MLG (red) and chirally twisted triple bilayer graphene (CTTBG, black) samples. The blue dashed line is the expected curve if the CTTBG sample has a single particle gap. (b) Picture of our CTTBG sample, which has local TG and global BG. (c) Landau fan of  $G$  data at zero perpendicular electric field. (d) The  $C$  and  $G$  components vs. the TG voltage at different  $B$ . The BG voltage is swept simultaneously to keep the perpendicular electric field at zero. The inset shows the expanded  $G$  near CNP where the triangle markers label two turning points. (e) Cartoons explaining our gap measurements. The red dotted lines represent the Fermi energy in graphene and the two gates. The DOS used in the cartoon is calculated for  $D = 0.047$  V/nm. The flat band condition is defined as  $V_{TG} = V_{BG} = 0$ .

the data read from oscillations at fields ranging from 0.5 to 2 T in Fig. 3(a), and calculates  $v_F$  from the slope of the linear relation  $\mu/n \propto 1/\sqrt{|n|}$ .  $v_F$  is  $0.89 \times 10^6$  m/s for holes and  $1.04 \times 10^6$  m/s for electrons. In principle, our analysis in Fig. 3(a) has no fitting parameters. It perfectly agrees with earlier STM studies, except that we can now have the graphene encapsulated between two gates [26–29]. This experimentally measured  $n$  vs. gate voltage relation is used in analyzing Fig. 2(b).

Once demonstrated the precision and reliability of this procedure, we now perform similar measurements on our CTTBG sample, see Fig. 3(a). The CTTBG sample has a local TG and a global BG, shown in Fig. 3(b). Using these two gates, we can independently manipulate the chemical potential  $\mu$  (and hence the carrier density  $n$ ) and the out-of-plane electric field, which is quantified as electric displacement  $D$  (V/nm). In Fig. 3(c-d), we show the  $G$  and  $C$  by sweeping the sample density while keeping zero  $D$ . Thanks to both the high quality of our sample and high sensitivity of the measurement, we are able to observe minima in both the  $C$  and  $G$  corresponding to integer Landau level filling factors at magnetic field as small as 0.5 T. Therefore, following the same procedure of MLG, we summarize the  $V_G/n$  using black symbols in Fig. 3(a). Unlike the linear dependence of  $V_G/n$  on  $1/\sqrt{n}$  seen in the MLG, we observe a constant  $V_G/n$  that is independent on the density, suggesting a constant  $\mu/n$  of either a parabolic dispersion or a diverging  $dn/d\mu$  for flat bands.

A gap-like feature, namely a minima in both the ca-

pacitance and conductance, appears at the CNP, see Fig. 3(d). The conductance minimum is flanked by two peaks, whose position coincides with the abrupt change of  $C$ . The gap size  $\Delta$  can be deduced from the gate voltage difference between the two  $G$  peaks as  $\Delta = \frac{2K}{1+K} \times \Delta V_{TG}$ . If  $\Delta$  is a single particle gap, the experimental data points are expected to match the blue dashed line. However, it is clearly not. Therefore, the gap seen in the experiment is likely a manifestation of many-body ferromagnetism, a signature that the interaction dominates over the kinetic energy. Therefore, the non-single-particle gap seen at CNP as well as the constant  $V_G/n$  strongly evidence the existence of a group of flat bands with different flavors [30].

The electric displacement  $D$  breaks the inversion symmetry of the system and induces a split  $\Delta_0$  between the flat bands with different valleys, see Fig. 3(e). The measurement principle can be explained by Fig. 3(e), which shows two configurations when the chemical potential  $\mu$  lies at the CNP and in the flat band, respectively [31]. Opposite gate voltage bias  $V_{TG} = -K^{-1}V_{BG}$  induces a finite  $D$  while keeping  $\mu$  unchanged, and non-zero  $V_{TG} + K^{-1}V_{BG}$  changes  $\mu$ . For example, Fig. 4(a) shows the  $C$  and  $G$  minima seen at the CNP when  $D = 0$  and  $-0.19$  V/nm. We summarize the measured  $\Delta_0$  as a function of  $D$  in Fig. 4(b). The experimental data points match the theoretical simulation (the solid line) at large  $D$ . However, a clear finite gap is seen at  $D = 0$ . As discussed earlier, the gap at  $D = 0$  is likely the spontaneous ferromagnetism stabilized by the dominating Coulomb

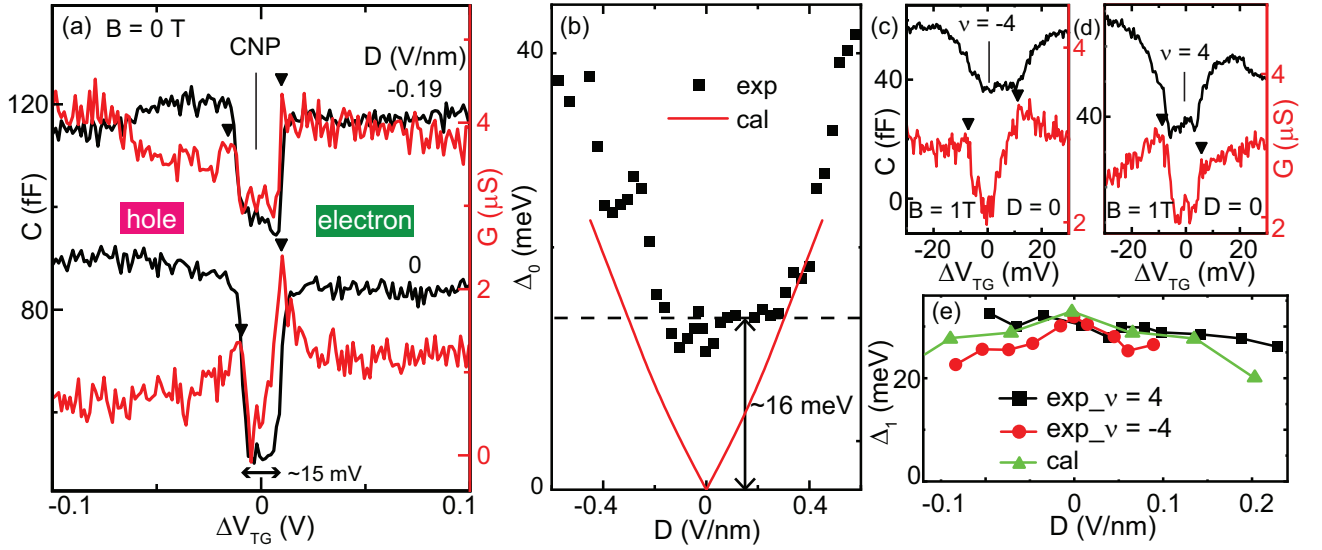


FIG. 4. (a)(c-d) The  $C$  and  $G$  components from the CTTBG sample near CNP at  $\nu = \pm 4$  and different  $D$  and  $B$  as labeled. Black triangles mark the turning points from which we determine the gaps. (b) The gaps at CNP extracted with different  $D$ . The red line shows the predicted gap by the continuum approximation. (e) Measured gaps at  $\nu = \pm 4$  and their predicted values at different  $D$ .

interaction. The  $G$  minimum exists and its width remains constant when a large magnetic field up to 10 T is applied, see in Fig. 3(c). It is worth mentioning that we observe no gap-feature at the CNP near  $D = 0$  in the transport study of this sample [12]. It is likely that because the gap seen in capacitance measurements are charging gaps, i.e. the discontinuity  $\mu$  as a function of  $n$ . Therefore, it is not in conflict with the existence of percolation process in domain structures [32].

The moiré flat bands are isolated from other dispersive bands by the superlattice strength. The moiré gaps  $\Delta_1$  in Fig. 3(e), are another important parameter of twistrionics materials, which is the separation between flat bands from higher energy dispersing bands.  $\Delta_1$  gradually decreases as electric field increases because electric field opens up the flat bands leading to the merging of flat bands and dispersive bands.  $\Delta_1$  corresponds to the  $\nu = \pm 4$  minimum in the  $C$  and  $G$  vs.  $V_G$  trace, inside which  $n$  remains constant and  $\mu$  varies through the gap, see Fig. 4(c-d). We mark the turning points flanking the  $G$  minima with black triangles, which is used as a measure of the minimum width. Fig. 4(e) summarizes the measured  $\Delta_1$  as a function of the  $D$  at  $\nu = \pm 4$ .  $\Delta_1$  gradually disappears as  $D$  increases. The experimentally measured results are in good agreement with the theoretical values, which validates our theoretical parameters used in this study.

In conclusion, capacitance measurement as a local compressibility probe has great advantage of revealing fine structure of two-dimensional systems. The deduced Fermi velocity of MLG is in agreement with previous results. Moreover, we study quantitative intrinsic band

structure of CTTBG. The inter-flat-band gap  $\Delta_0$  exists at zero perpendicular electric field, possibly induced by spontaneous ferromagnetism, which has never reported in such CTTBG moiré systems.

The work at PKU was supported by the National Key Research and Development Program of China (Grant No. 2021YFA1401900, 2019YFA0308402 and 2019YFA0308403), the Innovation Program for Quantum Science and Technology (Grant No. 2021ZD0302602 and 2021ZD0302403), and the National Natural Science Foundation of China (Grant No. 11934001, 92265106 and 11921005). J.-H.C acknowledges technical support from Peking Nanofab.

\* These authors contributed equally to this study.

† chenjianhao@pku.edu.cn

‡ xiaobolu@pku.edu.cn

§ liuyang02@pku.edu.cn

- [1] J. P. Eisenstein, L. N. Pfeiffer, and K. W. West, Compressibility of the two-dimensional electron gas: Measurements of the zero-field exchange energy and fractional quantum hall gap, *Phys. Rev. B* **50**, 1760 (1994).
- [2] E. M. Hajaj, O. Shtempluk, V. Kochetkov, A. Razin, and Y. E. Yaish, Chemical potential of inhomogeneous single-layer graphene, *Phys. Rev. B* **88**, 045128 (2013).
- [3] J. L. McChesney, A. Bostwick, T. Ohta, T. Seyller, K. Horn, J. González, and E. Rotenberg, Extended van hove singularity and superconducting instability in doped graphene, *Phys. Rev. Lett.* **104**, 136803 (2010).
- [4] S. L. Tomarken, Y. Cao, A. Demir, K. Watanabe, T. Taniguchi, P. Jarillo-Herrero, and R. C. Ashoori, Electronic compressibility of magic-angle graphene superlat-

- tices, Phys. Rev. Lett. **123**, 046601 (2019).
- [5] G. Li, A. Luican, J. M. B. Lopes dos Santos, A. H. Castro Neto, A. Reina, J. Kong, and E. Y. Andrei, Observation of van hove singularities in twisted graphene layers, Nature Physics **6**, 109 (2010).
- [6] S. L. Tomarken, Y. Cao, A. Demir, K. Watanabe, T. Taniguchi, P. Jarillo-Herrero, and R. C. Ashoori, Electronic compressibility of magic-angle graphene superlattices, Phys. Rev. Lett. **123**, 046601 (2019).
- [7] D. Weiss, K. V. Klitzing, K. Ploog, and G. Weimann, Magnetoresistance oscillations in a two-dimensional electron gas induced by a submicrometer periodic potential, Europhysics Letters **8**, 179 (1989).
- [8] M. Drienovsky, J. Joachimsmeier, A. Sandner, M.-H. Liu, T. Taniguchi, K. Watanabe, K. Richter, D. Weiss, and J. Eroms, Commensurability oscillations in one-dimensional graphene superlattices, Phys. Rev. Lett. **121**, 026806 (2018).
- [9] R. Bistritzer and A. H. MacDonald, Moiré bands in twisted double-layer graphene, Proceedings of the National Academy of Sciences **108**, 12233 (2011).
- [10] A. T. Pierce, Y. Xie, J. M. Park, E. Khalaf, S. H. Lee, Y. Cao, D. E. Parker, P. R. Forrester, S. Chen, K. Watanabe, T. Taniguchi, A. Vishwanath, P. Jarillo-Herrero, and A. Yacoby, Unconventional sequence of correlated chern insulators in magic-angle twisted bilayer graphene, Nature Physics **17**, 1210 (2021).
- [11] S. D. Sarma and A. Pinczuk, Perspectives in quantum hall effects: Novel quantum liquids in low-dimensional semiconductor structures (1997).
- [12] W. Wang, G. Zhou, W. Lin, Z. Feng, Y. Wang, M. Liang, Z. Zhang, M. Wu, L. Liu, K. Watanabe, T. Taniguchi, W. Yang, G. Zhang, K. Liu, J. Gao, Y. Liu, X. C. Xie, Z. Song, and X. Lu, Correlated charge density wave insulators in chirally twisted triple bilayer graphene, Phys. Rev. Lett. **132**, 246501 (2024).
- [13] T. Devakul, P. J. Ledwith, L.-Q. Xia, A. Uri, S. C. de la Barrera, P. Jarillo-Herrero, and L. Fu, Magic-angle helical trilayer graphene, Science Advances **9**, eadi6063 (2023).
- [14] L.-Q. Xia, S. C. de la Barrera, A. Uri, A. Sharpe, Y. H. Kwan, Z. Zhu, K. Watanabe, T. Taniguchi, D. Goldhaber-Gordon, L. Fu, T. Devakul, and P. Jarillo-Herrero, Helical trilayer graphene: a moiré platform for strongly-interacting topological bands, arXiv e-prints, arXiv:2310.12204 (2023), arXiv:2310.12204 [cond-mat.mes-hall].
- [15] R. T. Weitz, M. T. Allen, B. E. Feldman, J. Martin, and A. Yacoby, Broken-symmetry states in doubly gated suspended bilayer graphene, Science **330**, 812 (2010).
- [16] W. Bao, K. Myhro, Z. Zhao, Z. Chen, W. Jang, L. Jing, F. Miao, H. Zhang, C. Dames, and C. N. Lau, In situ observation of electrostatic and thermal manipulation of suspended graphene membranes, Nano Letters **12**, 5470 (2012).
- [17] M. Liang, M.-M. Xiao, Z. Ma, and J.-H. Gao, Moiré band structures of the double twisted few-layer graphene, Phys. Rev. B **105**, 195422 (2022).
- [18] See Supplemental Material for additional methods, data, and analyses.
- [19] For simplicity, we always define the gate bias  $V_G$  and the graphene chemical potential  $\mu$  in reference to the condition when the graphene is tuned to its CNP throughout this manuscript, see the black dash-dotted line in Fig. 1(c).
- [20] L. Zhao, W. Lin, X. Fan, Y. Song, H. Lu, and Y. Liu, High precision, low excitation capacitance measurement methods from 10 mK to room temperature, Review of Scientific Instruments **93**, 053910 (2022).
- [21] A. Hazegehi, J. A. Sulpizio, G. Diankov, D. Goldhaber-Gordon, and H. S. P. Wong, An integrated capacitance bridge for high-resolution, wide temperature range quantum capacitance measurements, Review of Scientific Instruments **82**, 053904 (2011).
- [22] Emergent dirac gullies and gully-symmetry-breaking quantum hall states in *aba* trilayer graphene, .
- [23] A. Assouline, T. Wang, H. Zhou, L. A. Cohen, F. Yang, R. Zhang, T. Taniguchi, K. Watanabe, R. S. K. Mong, M.-P. Zaletel, and A. F. Young, Energy gap of the even-denominator fractional quantum hall state in bilayer graphene, Phys. Rev. Lett. **132**, 046603 (2024).
- [24] B. E. Feldman, A. J. Levin, B. Krauss, D. A. Abanin, B. I. Halperin, J. H. Smet, and A. Yacoby, Fractional quantum hall phase transitions and four-flux states in graphene, Phys. Rev. Lett. **111**, 076802 (2013).
- [25] The  $C$  and  $G$  are highly entangled with each other [?]. Fortunately, this effect does not change our conclusion.
- [26] S. Y. Zhou, G. H. Gweon, J. Graf, A. V. Fedorov, C. D. Spataru, R. D. Diehl, Y. Kopelevich, D. H. Lee, S. G. Louie, and A. Lanzara, First direct observation of dirac fermions in graphite, Nature Physics **2**, 595 (2006).
- [27] G. Li and E. Y. Andrei, Observation of landau levels of dirac fermions in graphite, Nature Physics **3**, 623 (2007).
- [28] G. Li, A. Luican, and E. Y. Andrei, Scanning tunneling spectroscopy of graphene on graphite, Phys. Rev. Lett. **102**, 176804 (2009).
- [29] K.-K. Bai, Y.-C. Wei, J.-B. Qiao, S.-Y. Li, L.-J. Yin, W. Yan, J.-C. Nie, and L. He, Detecting giant electron-hole asymmetry in a graphene monolayer generated by strain and charged-defect scattering via landau level spectroscopy, Phys. Rev. B **92**, 121405 (2015).
- [30] The collective pinning of electron Wigner crystal may also lead to a gap-feature, however, it is rather courageous to suggest this senario in our sample. Also, the localization gap can also be excluded because our transport measurement shows no insulating behavior; see Fig. S5.
- [31] In Fig. 3(e), the electric field is kept to be constant, the gap size  $\Delta$  is tuned by two electrical gates simultaneously, so that the relation between  $\Delta$  and  $V_{TG}$  is  $\Delta = \frac{2K}{1+K} \times V_{TG}$  while if the gap size is only tuned by  $V_{TG}$ , the relation becomes  $\Delta = \frac{K}{1+K} \times V_{TG}$ .
- [32] E. P. De Poortere, E. Tutuc, and M. Shayegan, Critical resistance in the alas quantum hall ferromagnet, Phys. Rev. Lett. **91**, 216802 (2003).